

Finite beam elements based on Legendre polynomial expansions and node-dependent kinematics for the global-local analysis of composite structures

Original

Finite beam elements based on Legendre polynomial expansions and node-dependent kinematics for the global-local analysis of composite structures / Li, G.; de Miguel, A. G.; Pagani, A.; Zappino, E.; Carrera, E.. - In: EUROPEAN JOURNAL OF MECHANICS. A, SOLIDS. - ISSN 0997-7538. - 74:(2019), pp. 112-123.
[10.1016/j.euromechsol.2018.11.006]

Availability:

This version is available at: 11583/2722018 since: 2019-01-07T11:55:28Z

Publisher:

Elsevier

Published

DOI:10.1016/j.euromechsol.2018.11.006

Terms of use:

This article is made available under terms and conditions as specified in the corresponding bibliographic description in the repository

Publisher copyright

Elsevier postprint/Author's Accepted Manuscript

© 2019. This manuscript version is made available under the CC-BY-NC-ND 4.0 license
<http://creativecommons.org/licenses/by-nc-nd/4.0/>. The final authenticated version is available online at:
<http://dx.doi.org/10.1016/j.euromechsol.2018.11.006>

(Article begins on next page)

Finite beam elements based on Legendre polynomial expansions and node-dependent kinematics for the global-local analysis of composite structures

G. Li^a, A.G. de Miguel^a, A. Pagani^a, E. Zappino^{a,*}, E. Carrera^{a,b},

^a*MUL² Group, Department of Mechanical and Aerospace Engineering, Politecnico di Torino, Corso Duca degli Abruzzi 24, 10129 Torino, Italy.*

^b*Laboratory of Intelligent Materials and Structures, Tambov State Technical University, Sovetskaya 106, 392000 Tambov, Russia.*

Abstract

This article presents an approach to obtain refined beam models with optimal numerical efficiency. Hierarchical Legendre Expansions (HLE) and Node-dependent Kinematics (NDK) are used in combination to build efficient global-local FE models. By relating the kinematic assumptions to the selected FE nodes, kinematic refinement local to the nodes can be realized, and global-local models can be conveniently constructed. Without using any coupling approach or superposition of displacement field, beam models with NDK have compact and coherent formulations. Meanwhile, HLE is used in the local zone for the enrichment of the beam cross-sections to satisfy the requirement for high solution accuracy, leaving the global model with lower-order kinematic assumptions. Through the numerical investigation on slender laminated structures, it is demonstrated that the computational costs can be reduced significantly without losing numerical accuracy.

Keywords: refined beam theories, Carrera Unified Formulation, hierarchical Legendre expansions, node-dependent kinematics, finite element

1. Introduction

Composite structures are widely used in modern engineering nowadays, especially in the aerospace industry. Nevertheless, their heterogeneous properties give rise to significant challenges to numerical modeling. On the history of structural mechanics, a great variety of 1D
5 models for slender structures have been proposed. Classical theories such as Euler-Bernoulli

*Corresponding author. Tel: +39 0110906887, Fax: +39 0110906899.
Email address: enrico.zappino@polito.it (E. Zappino)

beam and Timoshenko beam (Timoshenko, 1922) are broadly applied in numerical methods, though they fail to give a precise approximation of the transverse stresses over the cross-sections of slender structures. Refined theories were suggested to overcome such a drawback. Vlasov (1984) suggested the warping functions to capture the cross-sectional warping of thin-walled structures. Schardt (1966) presented a Generalized Beam Theory (GBT) by expanding the displacement field with reference to the middle plane of the thin-walled beam. An interesting review of several of them was presented by Kapania and Raciti (1989a,b). Notably, the higher-order shear deformation theory proposed by Reddy (1984a,b) has been widely adopted in mechanical modeling as by Chikh et al. (2017) and successfully applied to the analysis of functionally graded materials as reported by Ebrahimi and Barati (2017), Ebrahimi and Farazmandnia (2017) and structures with graphene sheets by Ebrahimi and Shafiei (2017). A hyperbolic shear deformation theory was presented by Mahi et al. (2015).

Generally, the accuracy of the models can be improved by increasing the order of the mathematical functions used to describe the deformation of the beam cross-sections. Refined beam models can be developed in an asymptotic/axiomatic expansion approach (Carrera and Petrolo, 2011), for example, by using Mac Laurin's polynomials. Meanwhile, the increased number of expansions lead to raised degrees of freedom and more complex governing equations. Carrera (2002) proposed the Unified Formulation (CUF), which allows the governing equations of refined models to be attained in a compact and unified manner through the so-called fundamental nuclei (FNs). By increasing the order of the polynomials expanded on each cross-section, better approximation accuracy is promisingly to be achieved. In numerical analysis, the mathematical models can be refined until the prescribed accuracy is achieved. Also, by using general approximation functions, the stretching effects of laminated structures can be accounted, which might be important for some flexural responses as commented by Draiche et al. (2016).

Based on CUF, a variety of refined beam theories were applied to implement efficient beam finite elements (Carrera et al., 2014). CUF can incorporate both series expansions and interpolation polynomials to build refined beam models. A variety of refined theories can be implemented in the framework of CUF, including the classical Euler-Bernoulli and Timoshenko beams as well as the higher-order shear deformation theories. Equivalent Single Layer (ESL) models compute the integrals of the energy terms over the cross-section domain as a whole, and suit theories based on series expansions, such as Taylor, trigonometric, and hyperbolic series and so forth. Such models were put into practice by Carrera et al. (2013a) and Filippi et al. (2016). For refined beam elements using Layer-wise (LW) models, 2D-type discretization is used on the

cross-sectional domain for enrichment purposes. Since LW models can account for the physical
40 boundaries of each layer, the heterogeneity of the laminates can be appropriately considered.
Different sets of polynomials can be used as assumed deformations of the cross-sections, such
as the Lagrange-type Carrera et al. (2014) and the Chybeshev-type (Filippi et al., 2015) poly-
nomials. Recently, the hierarchical Legendre polynomial expansions (HLE) were introduced as
well for the refinement of kinematic assumption of beam models, as reported by Carrera et al.
45 (2017a). The adopted hierarchical functions for quadrilateral domains were inspired by Szabó
and Babuška (1991). Such hierarchical functions can trace back to the work of Peano (1976),
Szabó and Mehta (1978) and Zienkiewicz et al. (1983). In HLE models, the polynomial degree
remains as an independent input parameter, which makes a re-meshing on the cross-sections
unnecessary. Besides, HLE proves to be a useful tool in describing the exact geometrical bound-
50 aries of the cross-section domains for the refinement of the modes, as discussed by Pagani et al.
(2016).

The refinement of mathematical assumptions can improve the solution accuracy, but also
leads to an increased number of degrees of freedom in FE models, and possibly makes the solu-
tion computationally expensive. A local kinematic refinement can help to reach a compromise
55 between the desired accuracy and solution expenses. Local refinements can be defined on spe-
cific layers according to a global-local superposition hypothesis (Li and Liu, 1995, 1997). The
basic idea is to superimpose an LW displacement assumption defined on a specific layer to a
global component of ESL type. The underlying method is a multiple assumed displacement field
approach. Further investigations based this method were carried out by Chen and Wu (2005),
60 Chen and Si (2013), Khalili et al. (2014), and Lezgy-Nazargah et al. (2011). This approach is
further used to build adequate models that can facilitate the modeling of delamination, as put
forward by Williams (1999), Mourad et al. (2008), and Versino et al. (2014, 2015). An alter-
native method was suggested by Carrera et al. (2017d), who introduced through-the-thickness
variable kinematic capabilities to refined shell models. In their proposed method, the kinematic
65 assumptions were directly refined on the chosen layers as LW models, and the other layers will
be grouped and modeled as equivalent layers. D’Ottavio et al. (2016) suggested a similar con-
cept which was named as Sublaminar Generalized Unified Formulation (S-GUF). In these local
refinement approaches, though the LW kinematics have to be used over the entire planar domain
of the laminates, the requirement for 3D finite elements in ply grouping method (Chang et al.,
70 1990, Jones et al., 1984, Pagano and Soni, 1983, Sun and Liao, 1990) can be avoided.

A different local refinement scheme regards to the mesh discretization. The most direct

way is the h -version refinement, which increases the density of the mesh grids. Adaptive mesh-
 refinement was proposed to regenerate the mesh in the desired area based on an error estimator
 (Zienkiewicz and Zhu, 1987, Zhu and Zienkiewicz, 1988). Alternatively, p -version refinement
 75 increases the polynomial order of the element shape functions (Babuška et al., 1981, Surana
 et al., 2001, Szabó et al., 2004), consequently the numerical convergence performance can be
 improved. By augmenting the mesh density and element order at the same time, the h - p -
 version method combines the advantages of these two approaches (Babuška and Guo, 1988,
 Oden et al., 1989, Zienkiewicz et al., 1989, Reddy, 1993). The s -version refinement (Fish, 1992,
 80 Fish and Markolefas, 1992) improves the solution accuracy by superimposing an additional set of
 independent meshes on the existing FE model, which is also referred to as the mesh superposition
 technique. Still, this concept is based on the idea of multiple assumed displacement fields.
 Exploiting this approach, Reddy and Robbins (1994) and Robbins and Reddy (1996) suggested
 a so-called variable kinematic theory, which superimposed an ESL displacement field on a layer-
 85 wisely defined displacement field. Meanwhile, by employing the s -version refinement method,
 locally refined mesh with variable kinematics can be overlapped on the global mesh in which
 ESL assumptions are used. Consequently, the mathematical kinematic refinement and the mesh
 discretization refinement were both considered.

A variety of methods to couple an adequate global model to a locally refine one were proposed.
 90 By using Lagrangian multipliers to enforce the displacement compatibility at domain interfaces,
 the global model can be connected to a local one (Prager, 1967, Aminpour et al., 1995, Brezzi and
 Marini, 2005, Carrera et al., 2013b). This method is also known as the multi-point constraints or
 the three-field formulations. A multi-line approach was suggested by Carrera and Pagani (2013,
 2014) and Carrera et al. (2017b) for refined beam models, in which beam models with differ-
 95 ent orders were used for different layers along the beam-lines, and the interfacial displacement
 compatibility was ensured through Lagrange multipliers. The Arlequin method, proposed by
 Dhia (1998) and Dhia and Rateau (2005), can couple two models with incompatible kinematics
 and different mesh discretization through Lagrangian multipliers in an overlapping zone. This
 method has been adopted by many researchers in the analysis of multi-layered structures, like
 100 Biscani et al. (2011, 2012a,b), He et al. (2011), and Hu et al. (2008, 2010), to name but a few.
 A so-called eXtended Variational Formulation (XVF) with two Lagrange multipliers fields was
 proposed for the coupling of non-overlapping domains with different mathematical assumptions
 (Blanco et al., 2008, Wenzel et al., 2014). In a typical one-way sequential global-local method,
 the independent local model is driven by the displacement on the boundaries taken from a previ-

105 ously solved global problem (Muheim Thompson and Hayden Griffin JR, 1990). A drawback of
this method is that the influence of the local model on the global model is ignored. As a remedy,
iterative procedures were then proposed to achieve the equilibrium and compatibility at model
interfaces (Whitcomb and Woo, 1993a,b, Mao and Sun, 1991). In the meanwhile, the iterative
procedures usually consume extra computational resources. Further efforts towards the devel-
110 opment of two-way loose global-local coupling approaches were also reported by Hühne et al.
(2016) and Akterskaia et al. (2018).

Carrera and Zappino (2017) suggested an innovative approach for the construction of FE
models that can accommodate strong local effects in a natural and straightforward manner,
which was named as Node-dependent Kinematics (NDK). By relating cross-section functions to
115 the desired FE nodes, the kinematic assumptions attached to different nodes will contribute to
the element deformation capabilities through the shape functions. Elements with miscellaneous
nodal mathematical models can form a transition zone, bridging the refined local model to a
global model with low-order kinematics. Without using any additional coupling approaches nor
extra superposition techniques, NDK allows the construction of a simultaneous multi-kinematic
120 global-local FE model to be built conveniently. Thus, the compactness of the governing equations
is retained. NDK has been applied to build global-local models of multi-layered structures for
1D (Carrera et al., 2018a) and 2D (Zappino et al., 2017, Carrera et al., 2017c, Valvano and
Carrera, 2017) simulation. As a versatile approach, NDK was also used in the FE modeling of
piezo-patches (Carrera et al., 2017e, 2018b, Zappino et al., 2018).

125 In the present work, HLE is used as the displacement assumptions to generate refined beam
models and used in the framework of NDK. The combination of HLE kinematic models and NDK
lead to significantly improved numerical efficiency as well as convenience in the construction of
global-local FE models. Such an approach enables one to refine the kinematics locally at any
desirable node and improve the accuracy by simply increasing the polynomial degree of the
130 hierarchical functions. The related formulations are presented in the following sections. The
effectiveness of the proposed method is demonstrated through numerical examples on multi-
layered beam structures.

2. Refined beam element based on CUF

For a slender laminated structure shown in Figure 1, Let us consider that the longitudinal
direction is aligned along the y direction, the cross-section domain lies in the (x, z) plane. The

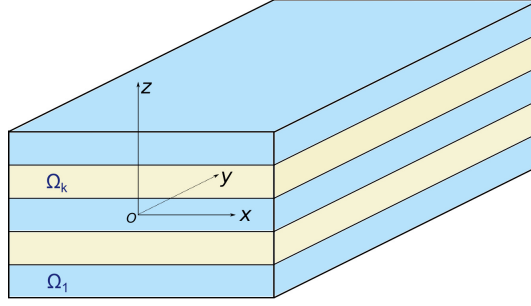


Figure 1: Reference system and notation of a laminated beam.

strain and stress components are herein arranged as:

$$\boldsymbol{\epsilon}^T = \{\epsilon_{xx}, \epsilon_{yy}, \epsilon_{zz}, \epsilon_{xz}, \epsilon_{yz}, \epsilon_{yx}\} \quad (1)$$

$$\boldsymbol{\sigma}^T = \{\sigma_{xx}, \sigma_{yy}, \sigma_{zz}, \sigma_{xz}, \sigma_{yz}, \sigma_{yx}\} \quad (2)$$

where the strain vector are related to the displacements through the differential operator matrix \mathbf{D} as:

$$\boldsymbol{\epsilon} = \mathbf{D}\mathbf{u} \quad (3)$$

For problems with infinitesimal strains, \mathbf{D} in an explicit form is:

$$\mathbf{D} = \begin{bmatrix} \frac{\partial}{\partial x} & 0 & 0 \\ 0 & \frac{\partial}{\partial y} & 0 \\ 0 & 0 & \frac{\partial}{\partial z} \\ \frac{\partial}{\partial z} & 0 & \frac{\partial}{\partial x} \\ 0 & \frac{\partial}{\partial z} & \frac{\partial}{\partial y} \\ \frac{\partial}{\partial y} & \frac{\partial}{\partial x} & 0 \end{bmatrix} \quad (4)$$

Meanwhile, the stresses and strains can be related through the constitutive equations:

$$\boldsymbol{\sigma} = \tilde{\mathbf{C}}\boldsymbol{\epsilon} \quad (5)$$

135 in which $\tilde{\mathbf{C}}$ is the matrix of material coefficients rotated from the material system to the analysis coordinate system shown in Figure 1.

In the framework of CUF, beam models are refined through the cross-section functions

$F_\tau(x, z)$, which lead to the following expression of the displacement field:

$$\mathbf{u}(x, y, z) = \mathbf{u}_\tau(y)F_\tau(x, z), \quad \tau = 1, \dots, M \quad (6)$$

where $\mathbf{u}_\tau(y)$ are the axial displacement unknown vectors, and M is the total number of expansions used in the cross-section functions $F_\tau(x, z)$. In FE discretization, the axial displacement vector can be approximated with Lagrangian shape functions and nodal unknowns as follows:

$$\mathbf{u}_\tau(y) = N_i(y)\mathbf{u}_{i\tau} \quad i = 1, \dots, N_n \quad (7)$$

in which $N_i(y)$ are the shape functions, and N_n the number of nodes within an element, $\mathbf{u}_{i\tau}$ the nodal unknowns. Thus, the complete expression of FE displacement functions formulated according to CUF can be written as:

$$\mathbf{u}(x, y, z) = N_i(y)F_\tau(x, z)\mathbf{u}_{i\tau}, \quad \tau = 1, \dots, M; \quad i = 1, \dots, N_n \quad (8)$$

It should be noted that, with the help of Einstein's summation convention, the displacement functions can be expressed in a compact form. The sub-indexes play an important role in describing various beam theories. CUF can account for the two modeling frameworks of laminated structures, namely ESL and LW models as illustrated in Figure 2. Beam theories based on higher-order Taylor series expansion (TE), according to the afore-described formulation, can be written as:

$$\begin{aligned} u_x &= u_{x_1} + xu_{x_2} + zu_{x_3} + x^2u_{x_4} + xzu_{x_5} + z^2u_{x_6} \\ u_y &= u_{y_1} + xu_{y_2} + zu_{y_3} + x^2u_{y_4} + xzu_{y_5} + z^2u_{y_6} \\ u_z &= u_{z_1} + xu_{z_2} + zu_{z_3} + x^2u_{z_4} + xzu_{z_5} + z^2u_{z_6} \end{aligned} \quad (9)$$

where:

$$F_1 = 1, \quad F_2 = x, \quad F_3 = z, \quad F_4 = x^2, \quad F_5 = xz, \quad F_6 = z^2 \quad (10)$$

For the Lagrange interpolation polynomial expansions (LE) defined on a quadrilateral domain (s, r) , a model based on four interpolation points (LE4) can be expressed as:

$$\begin{aligned} F_1 &= \frac{1}{4}(1 - \xi)(1 - \eta); & F_2 &= \frac{1}{4}(1 + \xi)(1 - \eta); \\ F_3 &= \frac{1}{4}(1 + \xi)(1 + \eta); & F_4 &= \frac{1}{4}(1 - \xi)(1 + \eta). \end{aligned} \quad (11)$$

in which $s, r \in [-1, 1]$, and $F_1(-1, -1) = 1$, $F_2(1, -1) = 1$, $F_3(1, 1) = 1$, $F_4(-1, 1) = 1$. LE-type cross-section functions expanded on nine points (LE9) can be defined accordingly.

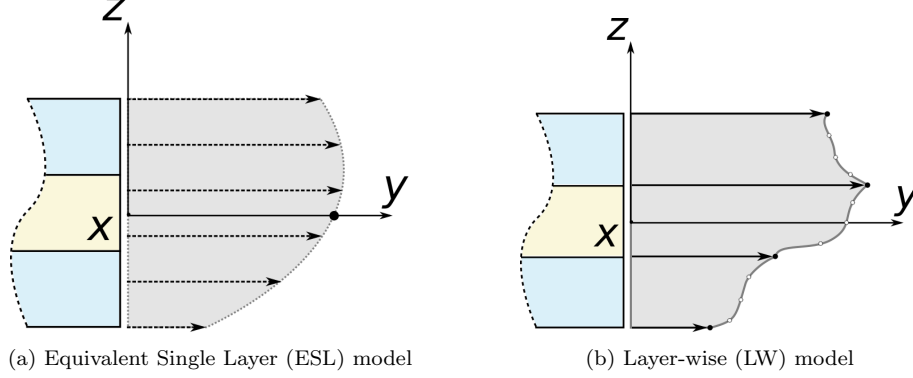


Figure 2: Two types of models for multi-layered structures.

3. Hierarchical Legendre Expansions (HLE) as cross-section functions

140 The cross-section functions can also be defined by Hierarchical Legendre Expansions (HLE).
 Inspired by the work of Szabó and Babuška (1991) and Szabó et al. (2004), HLE was employed for
 the refinement of beam models first by Pagani et al. (2016). Such type of cross-section functions
 treat the polynomial degree p as an independent variable. The functions for a quadrilateral
 domain (r, s) , defined for $[-1, 1]$, can be classified into vertex modes, side modes, and internal
 145 modes, as shown in Figure 3.

Vertex modes: These functions are defined as linear interpolations over the quadrilateral domain:

$$F_\tau(r, s) = \frac{1}{4}(1 - r_\tau r)(1 - s_\tau s) \quad \tau = 1, 2, 3, 4 \quad (12)$$

where r_τ and s_τ stand for the local isoparametric coordinates of point τ in a quadrilateral sub-domain with four points.

Side modes: Correspond to the edge-featuring modes, which are defined as:

$$\begin{aligned} F_\tau(r, s) &= \frac{1}{2}(1 - s)\phi_m(r) & \tau &= 5, 9, 13, 18, \dots \\ F_\tau(r, s) &= \frac{1}{2}(1 + r)\phi_m(s) & \tau &= 6, 10, 14, 19, \dots \\ F_\tau(r, s) &= \frac{1}{2}(1 + s)\phi_m(r) & \tau &= 7, 11, 15, 20, \dots \\ F_\tau(r, s) &= \frac{1}{2}(1 - r)\phi_m(s) & \tau &= 8, 14, 16, 21, \dots \end{aligned} \quad (13)$$

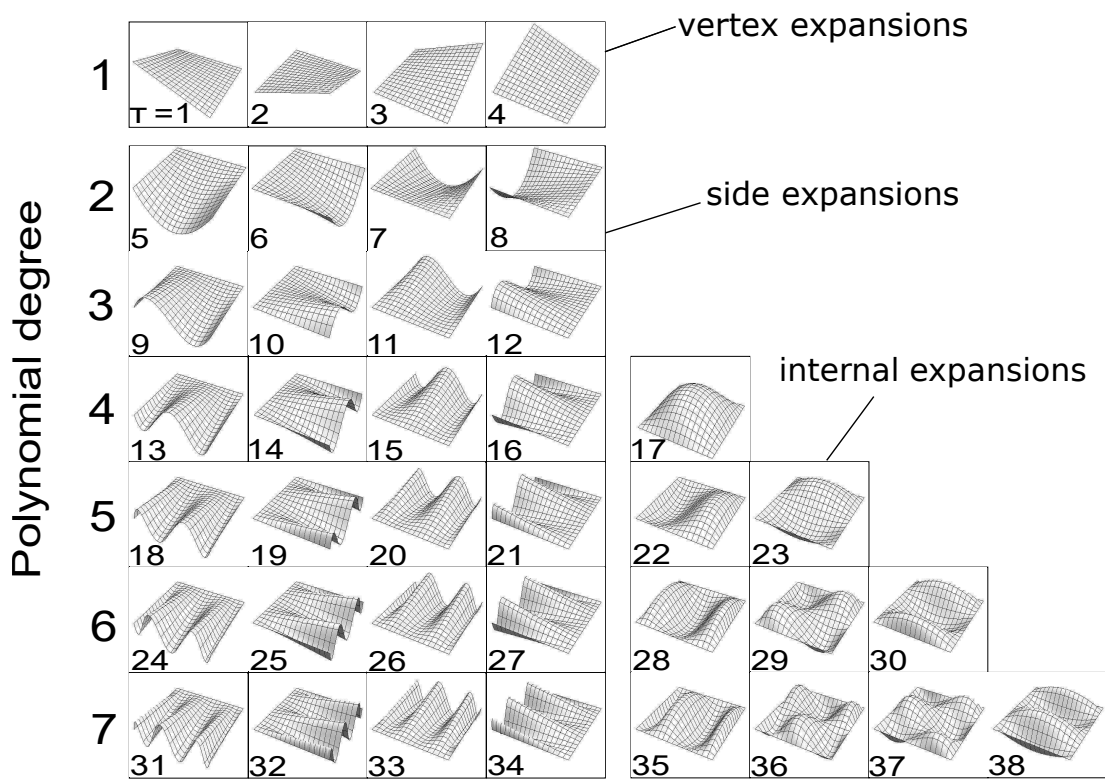


Figure 3: Hierarchical Legendre Expansions (HLE) as cross-section functions of refined beam models, with reference to Szabó and Babuška (1991).

where ϕ_m is expressed as follows:

$$\phi_m(r) = \sqrt{\frac{2m-1}{2}} \int_{-1}^r L_{m-1}(x) dx = \frac{L_m(r) - L_{m-2}(r)}{\sqrt{4m-2}} \quad m = 2, 3, \dots \quad (14)$$

Internal modes: Describe the deformation shapes happening on the internal surface which will vanish on the edges and vertexes, which are:

$$F_\tau(r, s) = \phi_m(r)\phi_n(s) \quad m, n \geq 2; \quad \tau = 17, 22, 23, 28, 29, 30, \dots \quad (15)$$

Since the set of functions for $p-1$ are contained in those for p , these type of functions are described as *hierarchical*. For a more detailed description, the reader is referred to Carrera et al. (2017a). The four vertexes are used to define the border of the quadrilateral domain on the cross-section of a beam model. In the LW framework, refined beam models using HLE can be formulated. Moreover, HLE can avoid the work in the re-allocation of interpolation points and the consequent re-definition of the functions. In a sense, HLE combines the advantages of Taylor series, i.e. hierarchical kinematics, and Lagrange interpolation polynomials, i.e. non-local distribution of unknowns.

4. Beam elements with Node-Dependent Kinematics (NDK)

In CUF-type displacement functions as in Equation 8, the cross-sections can be further related to its “anchoring” nodes i , leading to the following expression:

$$\mathbf{u}(x, y, z) = N_i(y)F_\tau^i(x, z)\mathbf{u}_{i\tau}, \quad \tau = 1, \dots, M_i; \quad i = 1, \dots, N_n \quad (16)$$

Equation 16 describes a family of 1D FE models with NDK. In such elements, each node can possess individually defined kinematics over the cross-section, then be interpolated by means of the nodal shape functions N_i over the element axial domain. As an example, Figure 4 shows a four-node beam with individual displacement assumptions on each node, and a kinematic transition is realized within this element. In this approach, a local kinematic refinement on the nodal level can be conveniently carried out.

The governing equations of NDK FE models can be derived from the principle of virtual displacements (PVD). For elastic bodies in static equilibrium, one has:

$$\delta L_{int} = \delta L_{ext} \quad (17)$$

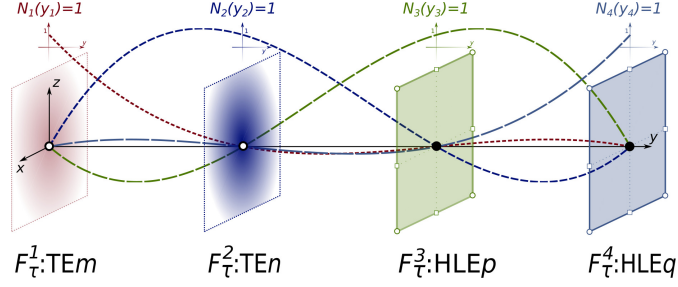


Figure 4: A B4 element with node-dependent kinematics.

where δL_{int} stands for internal work caused by the virtual deformations, and δL_{ext} represents the work done on the virtual displacements by the external forces. δL_{int} can be expressed as:

$$\delta L_{int} = \int_V \delta \boldsymbol{\epsilon}^T \boldsymbol{\sigma} dV \quad (18)$$

By invoking CUF-type displacement functions Equation 16, the geometric relations in Equation 3, and constitutive equations Equation 5, the following expression can be obtained:

$$\delta L_{int} = \delta \mathbf{u}_{js}^T \cdot \int_V N_j F_s^j \mathbf{D}^T \tilde{\mathbf{C}} \mathbf{D} F_\tau^i N_i dV \cdot \mathbf{u}_{i\tau} = \delta \mathbf{u}_{js}^T \cdot \mathbf{K}_{ij\tau s} \cdot \mathbf{u}_{i\tau} \quad (19)$$

where $\mathbf{K}_{ij\tau s}$ is the fundamental nucleus (FN) of stiffness matrix for NDK FE models. The explicit expression of $\mathbf{K}_{ij\tau s}$ reads:

$$\mathbf{K}_{ij\tau s} = \int_V N_j F_s^j \mathbf{D}^T \tilde{\mathbf{C}} \mathbf{D} F_\tau^i N_i dV \quad (20)$$

The virtual work δL_{ext} done by the external load \mathbf{p} is:

$$\delta L_{ext} = \int_V \delta \mathbf{u}^T \mathbf{p} dV \quad (21)$$

The above equation can be further written in the form of CUF as:

$$\delta L_{ext} = \delta \mathbf{u}_{js}^T \int_V N_j F_s^j \mathbf{p} dV = \delta \mathbf{u}_{js}^T \mathbf{P}_{js} \quad (22)$$

where \mathbf{P}^{js} represents the FN of the load vector. Hence, the governing equation for 1D FE models with NDK can be obtained as follows:

$$\delta \mathbf{u}_{js} : \quad \mathbf{K}_{ij\tau s} \cdot \mathbf{u}_{i\tau} = \mathbf{P}_{js} \quad (23)$$

For FE models with NDK, the assembly of the stiffness matrix and load vector can be carried out in a convenient and unified manner in the framework of CUF, as elaborated by Carrera and Zappino (2017) and Carrera et al. (2018a).
165

5. Numerical results and discussion

In this section, the capabilities of NDK when used in combination with HLE cross-section kinematics are investigated through two numerical examples:

- A simply supported sandwich beam under local pressure;
- 170 • A two-layered cantilever beam subjected to four points loads.

The first example demonstrates the capturing of local pressure concentration with NDK, and the second one presents the probing of structural responses in the region of interest. The accuracy of the solutions is compared against the computational consumption. The choice of the transition zone and the kinematics in the outlying area, as well as their influences on the efficiency, are discussed.
175

5.1. A simply supported sandwich beam under local pressure

A sandwich beam under local pressure is considered, which comprises two composite faces and a soft core as shown in Figure 5. The structure has the length $b = 10\text{mm}$, width $a = 2\text{mm}$, and total height $h = 2\text{mm}$, with layers of thickness $0.1h/0.8h/0.1h$. The material properties are as detailed in Table 1. Numerical studies on this case was also reported by Wenzel et al. (2014) and Zappino et al. (2017). In the present work, by making use of the symmetry features, a half of the structure is modeled. For the refined HLE beam elements used, the cross-section is meshed as presented in Figure 6, in which the three sub-domains are approximated by the same set of HLE p cross-section functions, respectively. According to the results in Table 2, FE model with 20 B4 elements along the axial direction can give a satisfactory approximation. The HLE refinement is first assessed by increasing the polynomial order p until 7. Then FE models constructed with NDK are employed in the analysis. The obtained displacements and stresses are summarized in Table 2. Solutions achieved with pure TE and LE kinematics are listed for comparison.
180
185

In Table 2, with the increase of the polynomial order of the kinematic assumption on the beam cross-section, the numerical results converge gradually. In terms of σ_{zz} , the theoretical solution is -1 MPa on the loaded surface, and all the HLE models can achieve fairly good accuracy. The
190

Table 1: Material properties used on the sandwich beam.

	E_{11} [GPa]	E_{22} [GPa]	E_{33} [GPa]	ν_{12}	ν_{13}	ν_{23}	G_{12} [GPa]	G_{13} [GPa]	G_{23} [GPa]
Face	131.1	6.9	6.9	0.32	0.32	0.49	3.588	3.088	2.3322
Core	0.2208×10^{-3}	0.2001×10^{-3}	2.76	0.99	0.00003	0.00003	16.56×10^{-3}	0.5451	0.4554

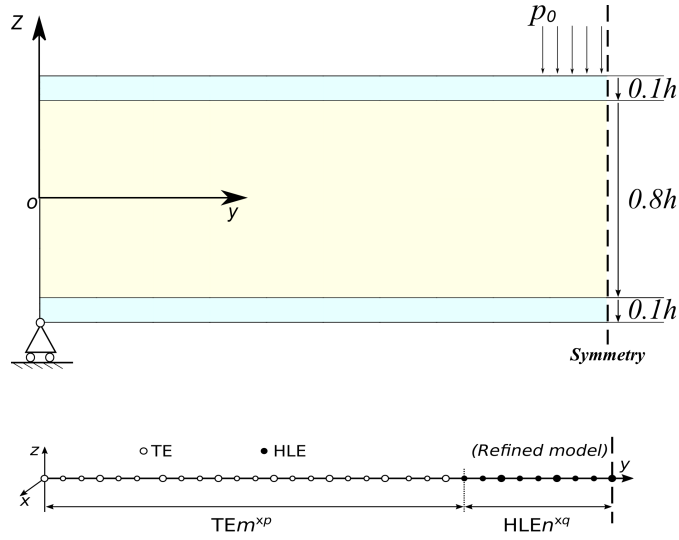


Figure 5: Geometry and FE model of the sandwich beam.

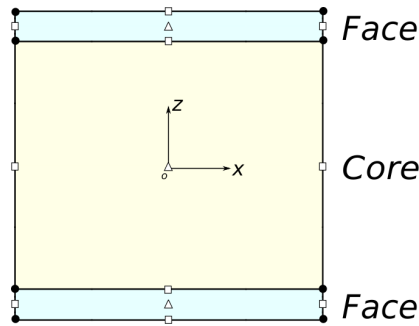


Figure 6: Mesh on the cross-section of the sandwich beam: 3 sub-domains, each with HLE p .

through-the-thickness variation of σ_{yz} obtained with HLE kinematics of different orders are as shown in Figure 7(a). Due to the low stiffness, the core has much lower stress gradients than the faces of the sandwich. It can be observed that, HLE2 fails to capture the variation of σ_{yz} through the two faces of the sandwich. From HLE3 to HLE7, σ_{yz} shows converged distribution through the sandwich thickness, and zero transverse shear stress on the free surfaces is progressively approached. In fact, HLE3 can already satisfy the accuracy requirement of engineering practice. The relative error of σ_{yz} given by different kinematics (with respect to HLE7 solution) are plotted versus the degrees of freedom in Figure 7(b). Even if the curve of relative error is not monotonically decreasing, the overall trend exhibits a convergence pattern. On the other hand, this curve shows the possibility of improving the accuracy by further increasing the polynomial order, yet it may not be necessary considering the computational efforts.

Table 2: Displacement and stress evaluation on the sandwich beam under local pressure.

Mesh	Kinematics	$-w[10^{-3}\text{mm}]$ $(0, \frac{b}{2}, -\frac{h}{2})$	$-\sigma_{yy}[\text{MPa}]$ $(0, \frac{b}{2}, \frac{h}{2})$	$-\sigma_{yz}[\text{MPa}]$ $(\frac{a}{2}, \frac{9b}{20}, \frac{9h}{20})$	$-\sigma_{zz}[\text{MPa}]$ $(0, \frac{b}{2}, \frac{h}{2})$	DOFs
B4×10	HLE2	2.467	17.72	0.8339	1.097	1674
B4×20	HLE2	2.467	17.77	0.8164	1.015	3294
B4×20	HLE3	2.469	18.33	1.062	1.048	5124
B4×20	HLE4	2.469	18.14	1.083	0.9965	7503
B4×20	HLE5	2.469	18.11	1.060	0.9884	10431
B4×20	HLE6	2.469	18.24	1.079	0.9789	13908
B4×20	HLE7	2.469	18.24	1.094	0.9771	17934
B4×20	TE1	1.515	7.300	1.163	0.9547	549
B4×20	TE3	2.309	17.52	0.8777	1.502	1830
B4×20	TE5	2.338	17.25	0.8815	0.7839	3843
B4×20	TE1 ^{×49} -HLE7 ^{×12}	1.547	15.63	1.437	0.9791	3969
B4×20	TE1 ^{×31} -HLE7 ^{×30}	1.820	18.07	1.112	0.9772	9099
B4×20	TE3 ^{×31} -HLE7 ^{×30}	2.376	18.23	1.096	0.9771	9750
B4×20	TE5 ^{×31} -HLE7 ^{×30}	2.388	18.23	1.096	0.9771	10773
B4×20	TE7 ^{×31} -HLE7 ^{×30}	2.419	18.24	1.095	0.9771	12168
Zappino et al. (2017)(2D)		2.471	18.11	1.180	0.9989	37479

HLE7 is further used together with TE kinematics to build FE models through NDK. In the region containing and near the loaded zone, HLE7 is applied on the beam cross-section, and the rest of the beam is modeled with TE-type theories. The FE models with NDK are indicated by TE $m^{\times p}$ -HLE7 $^{\times q}$, where m signifies the order of the TE model used, while p and q represent the numbers of nodes adopting the corresponding kinematics. For the FE models with 20 B4 elements, there are 61 nodes in total along the beam axis. As explained in previous sections, in the proposed approach, the transition zone in the global-local model covers the range of one

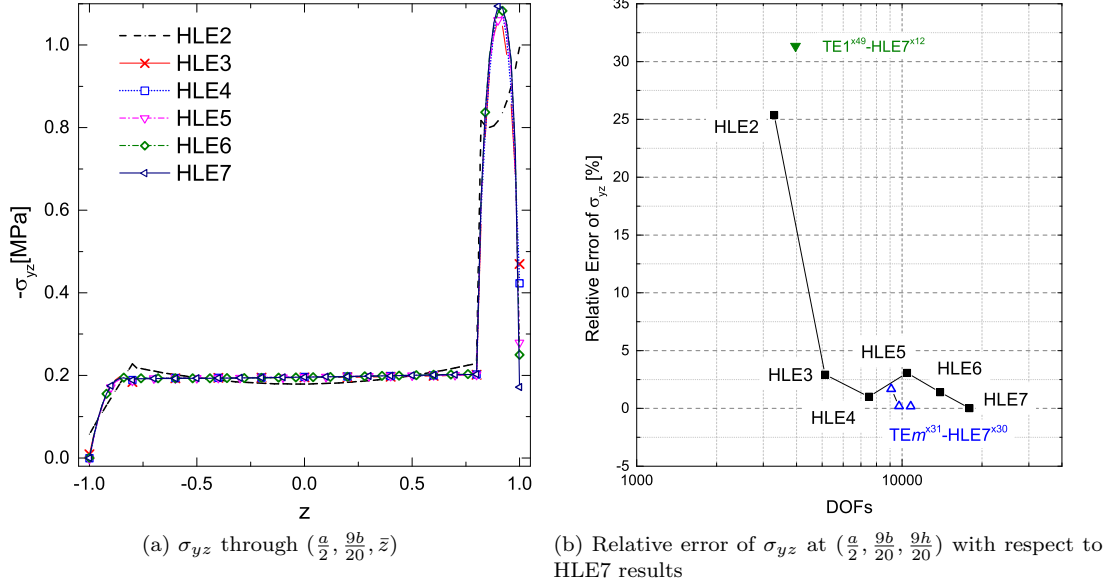


Figure 7: Evaluation of σ_{yz} on the sandwich beam under local pressure.

element. In this section, two locations for the transition zone are examined. Transition zone α is located around 75% length of the beam which leads to NDK model $TEm^{\times 49}$ -HLE7 $^{\times 12}$. While transition zone β is placed near 50% of the length range and corresponds to models denoted by $TEm^{\times 31}$ -HLE7 $^{\times 30}$.

215 Concerning the σ_{yz} as illustrated in Figure 7(b), the NDK models with the transition zone β yield comparable accuracy with a pure HLE7 model at a reduced number of degrees of freedom, but results achieved by $TEm^{\times 49}$ -HLE7 $^{\times 12}$ is far from satisfaction. From the comparison of the displacement and stress evaluation in Table 2 and Figure 8, it can be observed that $TE1^{\times 31}$ -HLE7 $^{\times 30}$ has better accuracy than $TE1^{\times 49}$ -HLE7 $^{\times 12}$ within the faces. This reality implies that
 220 transition zone β , which is further away from the zone with local effects, is more proper than transition zone α . In the meanwhile, in $TEm^{\times 31}$ -HLE7 $^{\times 30}$ models, the increase of TE kinematic order m further helps to improve the solution accuracy at the expense of extra computational effort. Regarding the transverse shear stress σ_{yz} , given that TE5 fails to capture its variation well, $TE1^{\times 31}$ -HLE7 $^{\times 30}$ already leads to results with fairly good accuracy. At the same time,
 225 compared with FE model with pure HLE7 kinematics, a 49% reduction in the number of degrees of freedom is also achieved by $TE1^{\times 31}$ -HLE7 $^{\times 30}$. It should be noted that the cost of the reduced computational consumption is some loss in the accuracy of the displacement solution.

Figure 9 shows the variation of w , σ_{yy} and σ_{yz} along the beam axial direction. Notably, an

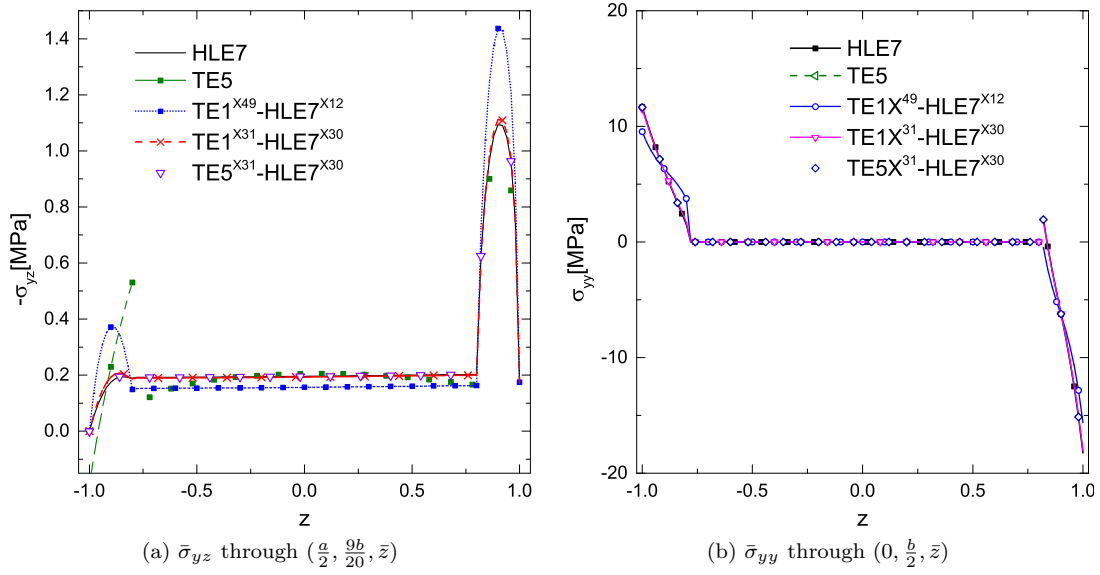
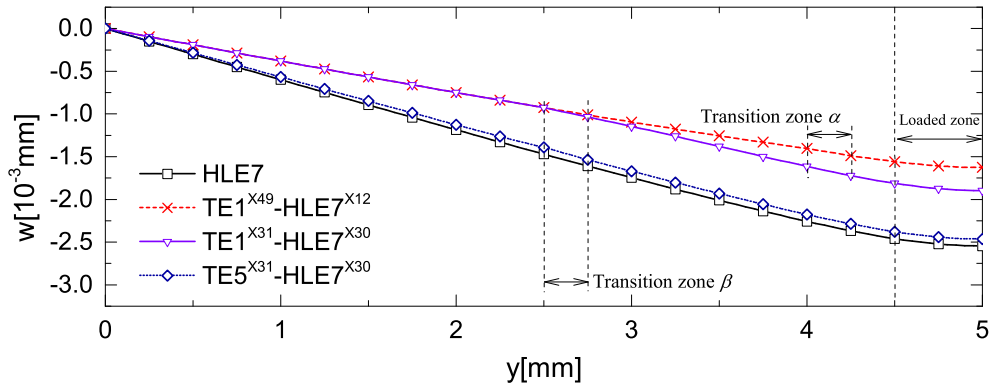


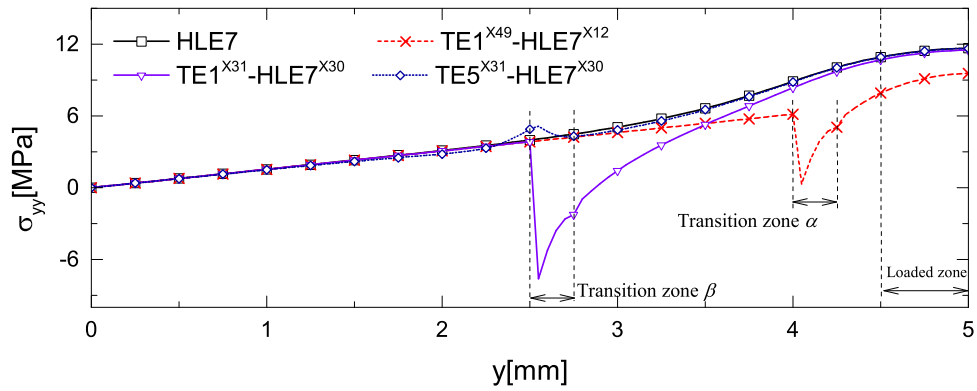
Figure 8: Through-the-thickness variation of $\bar{\sigma}_{yz}$ and $\bar{\sigma}_{yy}$ on the sandwich beam under local pressure.

oscillation exists in the stress distribution within and nearby the transition zone, although no
 230 transition effects are observed in the displacement solutions. Considering σ_{yy} and σ_{yz} in the
 loaded zone, by taking HLE7 solutions as references, TE1^{X31}-HLE7^{X30} leads to better results
 compared with the other models. This fact shows that transition zone β is more appropriately
 chosen than transition zone α . Meanwhile, with the refinement of the TE theories, the stress
 oscillation can be mitigated considerably, and the accuracy of both the displacement and stresses
 235 is improved.

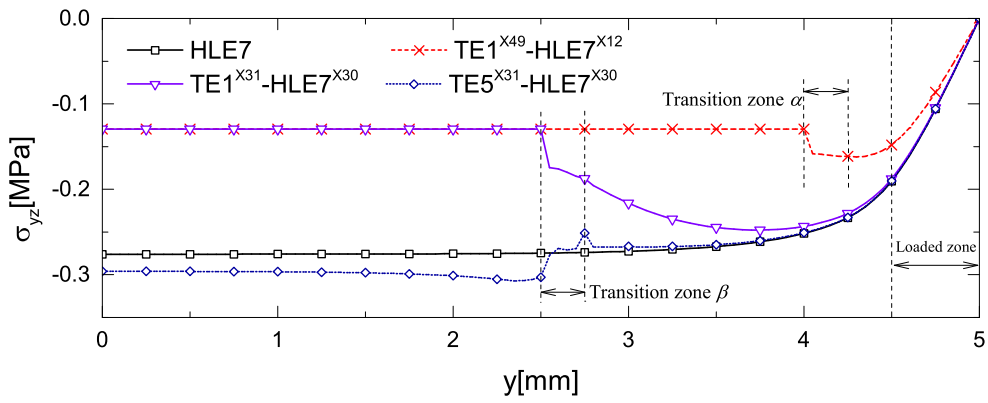
The contour of σ_{yz} and σ_{zz} obtained with model HLE7 and TE5^{X31}-HLE7^{X30} are compared
 in Figure 10 and Figure 11, respectively. As a result of the local pressure, significant stress
 concentration occurs on the right-hand side, especially within the upper face of the sandwich.
 The stress oscillation can also be observed in the vicinity of the transition zone. Such effects in
 240 models with incompatible kinematics were also reported by (Wenzel et al., 2014) about eXtended
 Variational Formulation, and by (Zappino et al., 2017, Carrera et al., 2018a) in NDK approaches.
 Even though, in the local region including the loaded zone, the stress fields obtained with the
 two models agree well with each other. In conclusion, compared with the pure HLE7 model, the
 NDK model TE5^{X31}-HLE7^{X30} is capable of capturing satisfactory displacement and stress field
 245 with a much fewer number of degrees of freedom.



(a) \bar{w} along $(0, y, 0)$



(b) $\bar{\sigma}_{yy}$ along $(0, y, -\frac{h}{2})$



(c) $\bar{\sigma}_{yz}$ along $(0, y, 0)$

Figure 9: Variation of σ_{yy} and σ_{yz} along the axial direction of the sandwich beam.

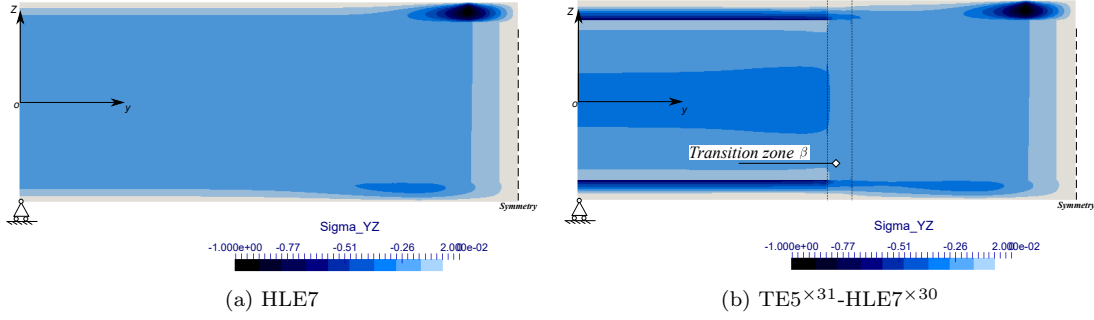


Figure 10: Contour plot of σ_{yz} on surface $(\frac{a}{2}, y, z)$ of the sandwich beam under local pressure.

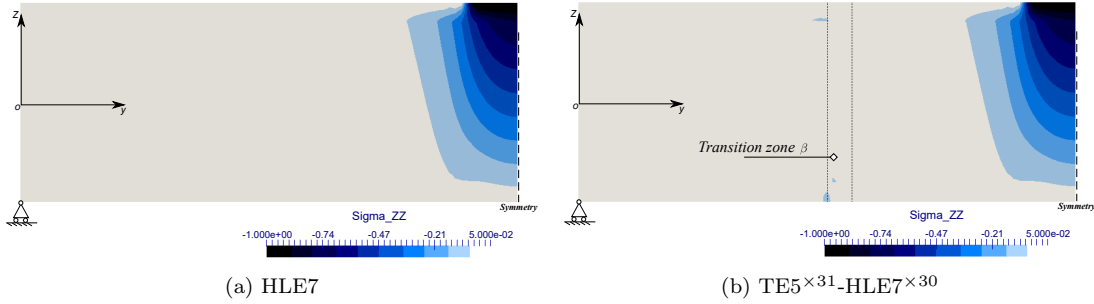


Figure 11: Contour plot of σ_{zz} on surface $(\frac{a}{2}, y, z)$ of the sandwich beam under local pressure.

5.2. A two-layered cantilever beam under four points loads

As the second example, a cantilever beam with two layers is analyzed using the NDK approach. The beam is clamped on one end and subjected to four point loads at the vertexes on the loading end. Geometrical features of the structure are shown in Figure 12, with length $b = 0.09\text{m}$, width $a = 0.001\text{m}$, and height $h = 0.01\text{m}$. The two layers are of equal thickness ($t = h/2$), both with the longitudinal direction along the beam axial direction y . The lower layer is made of Material 1, and the upper one of Material 2. Elastic properties of the materials are listed in Table 3, in which L and T stand the longitudinal and transverse direction of the fibers, respectively. The structure is discretized into a number of B4 elements as in shown Figure 12.

Models with complete HLE kinematics are first analyzed, in which the polynomial order p is increased until a numerical convergence is achieved. Then, to reduce the computational costs, in the area distant from the loaded region on the clamped side, TE kinematics is introduced, leading to NDK models $\text{TE1}^{\times 49}\text{-HLE7}^{\times 12}$ and $\text{TE1}^{\times 31}\text{-HLE7}^{\times 30}$. The superscripts represent the number of nodes with the corresponding kinematics. $\text{TE1}^{\times 49}\text{-HLE7}^{\times 12}$ has the transition zone

260 near 75% position along the axis away from the clamped end, and $TE1^{\times 31}$ -HLE7 $\times 30$ has it near the mid-span position.

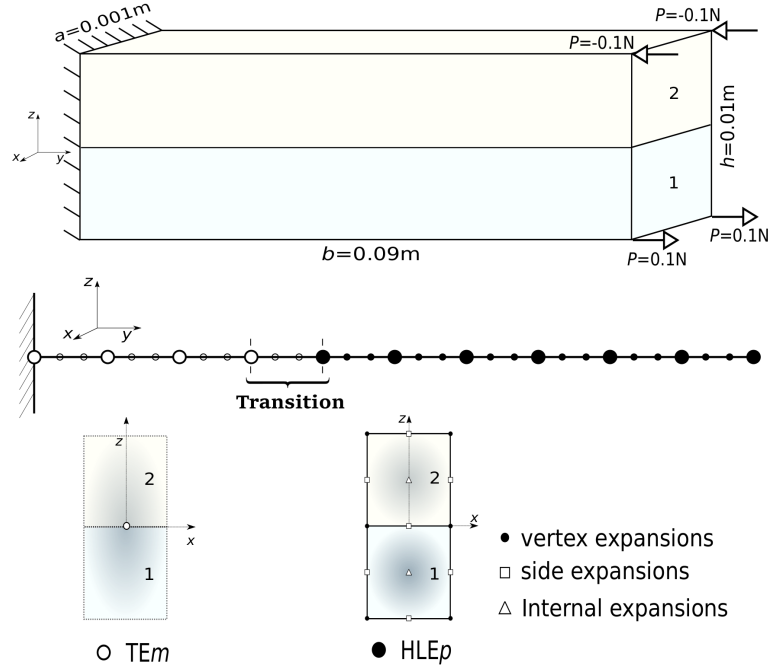


Figure 12: Geometry features and FE model of the two-layered cantilever beam (not to scale).

Table 3: Properties of the materials used for the two-layered cantilever beam.

	E_L [GPa]	E_T [GPa]	ν_{LT}	G_{LT} [GPa]
Material-1	30	1	0.25	0.5
Material-2	5	1	0.25	0.5

From the results summarized in Table 4, it can be noticed that with 20 B4 elements using pure HLE kinematics, the numerical convergence can be reached when HLE5 is employed. Besides, the transverse shear stress σ_{yz} is the critical case concerning the convergence. The convergence process can also be observed from the variation of σ_{yz} through the thickness along $(0, \frac{8b}{9}, \bar{z})$, as shown in Figure 13. The σ_{yz} shows a complex distribution due to the anisotropy and thickness effects. The obtained solutions are in good agreement with those given by the ABAQUS 3D model, which uses $4 \times 180 \times 32$ ($x \times y \times z$) quadratic brick elements with reduced integration (C3DR20).

270 If TE1 kinematics is employed on the left-hand side of the structure, a considerable reduction in the total degrees of freedom can be achieved, which is 65% for $TE1^{\times 31}$ -HLE7 $\times 30$, and 49%

for $\text{TE1}^{\times 49}\text{-HLE7}^{\times 12}$. According to the results in Table 4 and the stress variation in Figure 14, $\text{TE1}^{\times 31}\text{-HLE7}^{\times 30}$ has better accuracy compared to model $\text{TE1}^{\times 49}\text{-HLE7}^{\times 12}$ regarding the transverse shear stress σ_{yz} . These effects also confirm that transition zone β is a more decent choice. Though, both of the two models lead to reasonable evaluations. In engineering practice, if the transition zone lies outside the critical region, it may not be worthy of extra efforts to take the stress oscillation into account.

Table 4: Displacement and stress evaluation on the two-layered cantilever beam.

Mesh	Kinematics	$w[10^{-3}\text{mm}]$ $(0, b, 0)$	$\sigma_{yy}[\text{KPa}]$ $(0, \frac{8b}{9}, -\frac{h}{2})$	$\sigma_{yz}[\text{KPa}]$ $(0, \frac{8b}{9}, -\frac{h}{4})$	DOFs
B4×10	HL2	9.041	236.6	2.563	1209
B4×20	HL2	9.036	234.0	2.610	2379
B4×20	HL3	9.082	245.1	4.518	3660
B4×20	HL4	9.065	236.4	4.432	5307
B4×20	HL5	9.075	233.4	4.972	7320
B4×20	HL6	9.063	233.8	4.986	9699
B4×20	HL7	9.074	234.8	4.972	12444
B4×20	TE1	9.053	215.1	0.000	549
B4×20	$\text{TE1}^{\times 49}\text{-HLE7}^{\times 12}$	9.120	234.0	4.294	2889
B4×20	$\text{TE1}^{\times 31}\text{-HLE7}^{\times 30}$	9.117	234.8	4.970	6399
ABAQUS (3D)		9.071	235.3	4.963	337251

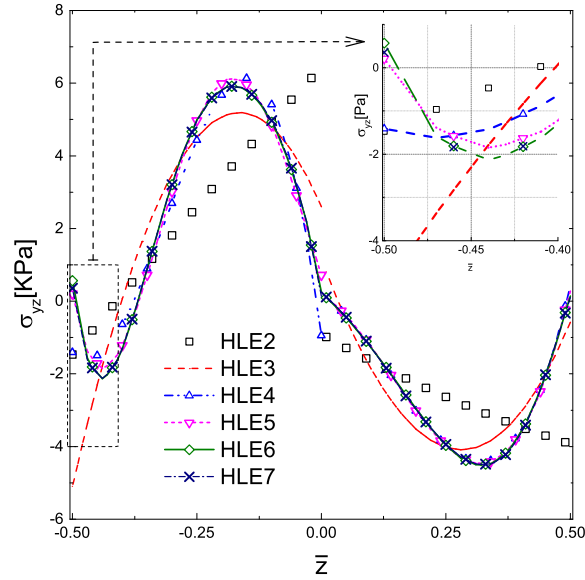


Figure 13: Variation of σ_{yz} along $(0, \frac{8b}{9}, \bar{z})$ on the two-layered cantilever beam, obtained with HLE models.

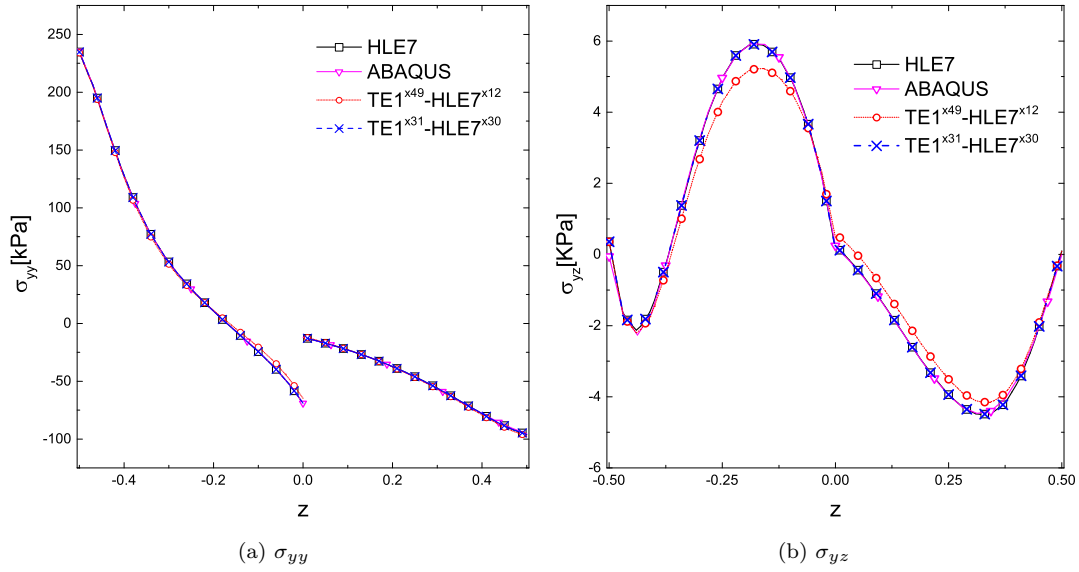


Figure 14: Variation of σ_{yy} and σ_{yz} along $(0, \frac{8b}{9}, \bar{z})$ on the two-layered cantilever beam, obtained with various models.

6. Conclusions

This work presents a class of refined 1D FE models with node-dependent kinematics for the global-local analysis of composite laminated beam structures. Hierarchical Legendre Expansions (HLE) are adopted as cross-section functions for the local refinement on the nodal level. By treating the polynomial degree p as an input parameter, and assigning refined kinematics to the desirable nodes in the local zone of interest, a series of FE models can be built conveniently when the FE meshes have been chosen. Such an approach can help to improve the numerical efficiency in engineering simulations and simplifies the modeling procedure. It can be highlighted that:

- Node-dependent kinematics provides a solution to integrate the accuracy of LW models and the low computational cost of ESL models and therefore, provides optimal beam models;
- The combination of HLE and NDK improves the computational efficiency of FE models for the analysis of multi-layered slender structures;
- Based on CUF, the compactness of the FE formulations is assured by using no additional coupling nor superposition;

- The presented approach allows the local kinematic refinement to be carried out without changing the FE mesh.

295 As future work, implementing an adaptive nodal-kinematic refinement routine will help to further enhance the efficiency of FE models with the least user intervention. And, more realistic cases of engineering interest can be considered.

7. Acknowledgment

This research work has been carried out within the project FULLCOMP (FULLy analysis, 300 design, manufacturing, and health monitoring of COMposite structures), funded by the European Union Horizon 2020 Research and Innovation program under the Marie Skłodowska Curie grant agreement No. 642121. E. Carrera acknowledges the Russian Science Foundation under grant No. 18-19-00092.

References

- 305 M. Akterskaia, E. Jansen, S. Hühne, and R. Rolfes. Efficient progressive failure analysis of multi-stringer stiffened composite panels through a two-way loose coupling global-local approach. *Composite Structures*, 183(Supplement C):137 – 145, 2018. ISSN 0263-8223. In honor of Prof. Y. Narita.
- M. A. Aminpour, J. B. Ransom, and S. L. McCleary. A coupled analysis method for structures 310 with independently modelled finite element subdomains. *International Journal for Numerical Methods in Engineering*, 38(21):3695–3718, 1995.
- I. Babuška and B. Guo. The h-p version of the finite element method for domains with curved boundaries. *SIAM Journal on Numerical Analysis*, 25(4):837–861, 1988.
- I. Babuška, B. A. Szabó, and I. N. Katz. The p-version of the finite element method. 315 *SIAM Journal on Numerical Analysis*, 18(3):515–545, 1981.
- F. Biscani, G. Giunta, S. Belouettar, E. Carrera, and H. Hu. Variable kinematic beam elements coupled via Arlequin method. *Composite Structures*, 93(2):697–708, 2011.
- F. Biscani, G. Giunta, S. Belouettar, E. Carrera, and H. Hu. Variable kinematic plate elements 320 coupled via Arlequin method. *International Journal for Numerical Methods in Engineering*, 91(12):1264–1290, 2012a.

- F. Biscani, P. Nali, S. Belouettar, and E. Carrera. Coupling of hierarchical piezoelectric plate finite elements via Arlequin method. *Journal of Intelligent Material Systems and Structures*, 23(7):749–764, 2012b.
- P. Blanco, R. Feijóo, and S. Urquiza. A variational approach for coupling kinematically incompatible structural models. *Computer Methods in Applied Mechanics and Engineering*, 197(17):1577–1602, 2008.
- F. Brezzi and L. D. Marini. The three-field formulation for elasticity problems. *GAMM-Mitteilungen*, 28(2):124–153, 2005.
- E. Carrera. Theories and finite elements for multilayered, anisotropic, composite plates and shells. *Archives of Computational Methods in Engineering*, 9(2):87–140, 2002.
- E. Carrera and A. Pagani. Analysis of reinforced and thin-walled structures by multi-line refined 1d/beam models. *International Journal of Mechanical Sciences*, 75:278–287, 2013.
- E. Carrera and A. Pagani. Multi-line enhanced beam model for the analysis of laminated composite structures. *Composites Part B: Engineering*, 57:112–119, 2014.
- E. Carrera and M. Petrolo. On the effectiveness of higher-order terms in refined beam theories. *Journal of Applied Mechanics*, 78(2):1–17, 2011.
- E. Carrera and E. Zappino. One-dimensional finite element formulation with node-dependent kinematics. *Computers & Structures*, 192:114–125, 2017.
- E. Carrera, M. Filippi, and E. Zappino. Laminated beam analysis by polynomial, trigonometric, exponential and zig-zag theories. *European Journal of Mechanics-A/Solids*, 41:58–69, 2013a.
- E. Carrera, A. Pagani, and M. Petrolo. Use of Lagrange multipliers to combine 1D variable kinematic finite elements. *Computers & Structures*, 129:194–206, 2013b.
- E. Carrera, M. Cinefra, M. Petrolo, and E. Zappino. *Finite element analysis of structures through Unified Formulation*. John Wiley & Sons, 2014.
- E. Carrera, A. G. de Miguel, and A. Pagani. Hierarchical theories of structures based on Legendre polynomial expansions with finite element applications. *International Journal of Mechanical Sciences*, 120:286–300, 2017a.

- 350 E. Carrera, M. Filippi, A. Pagani, and E. Zappino. Node-dependent kinematics, refined zig-zag and multi-line beam theories for the analysis of composite structures. In *58th AIAA/ASCE/AHS/ASC Structures, Structural Dynamics, and Materials Conference*, page 0425, 2017b.
- E. Carrera, A. Pagani, and S. Valvano. Multilayered plate elements accounting for refined theories and node-dependent kinematics. *Composites Part B: Engineering*, 114:189–210, 2017c.
- 355 E. Carrera, A. Pagani, and S. Valvano. Shell elements with through-the-thickness variable kinematics for the analysis of laminated composite and sandwich structures. *Composites Part B: Engineering*, 111:294–314, 2017d.
- E. Carrera, S. Valvano, and G. M. Kulikov. Multilayered plate elements with node-dependent kinematics for electro-mechanical problems. *International Journal of Smart and Nano Materials*, pages 1–39, 2017e.
- 360 E. Carrera, E. Zappino, and G. Li. Finite element models with node-dependent kinematics for the analysis of composite beam structures. *Composites Part B: Engineering*, 132(Supplement C):35 – 48, 2018a. ISSN 1359-8368.
- E. Carrera, E. Zappino, and G. Li. Analysis of beams with piezo-patches by node-dependent kinematic finite element method models. *Journal of Intelligent Material Systems and Structures*, 29(7):1379–1393, 2018b.
- 365 F.-K. Chang, J. L. Perez, and K.-Y. Chang. Analysis of thick laminated composites. *Journal of Composite Materials*, 24(8):801–822, 1990.
- W. Chen and J. Si. A model of composite laminated beam based on the global–local theory and new modified couple-stress theory. *Composite Structures*, 103:99–107, 2013.
- 370 W. Chen and Z. Wu. A new higher-order shear deformation theory and refined beam element of composite laminates. *Acta Mechanica Sinica*, 21(1):65–69, 2005.
- A. Chikh, A. Tounsi, H. Hebali, and S. Mahmoud. Thermal buckling analysis of cross-ply laminated plates using a simplified hsdt. *Smart Structures and Systems*, 19(3):289–297, 2017.
- 375 H. B. Dhia. Multiscale mechanical problems: the Arlequin method. *Comptes Rendus de l’Academie des Sciences Series IIB Mechanics Physics Astronomy*, 12(326):899–904, 1998.

- H. B. Dhia and G. Rateau. The Arlequin method as a flexible engineering design tool. *International Journal for Numerical Methods in Engineering*, 62(11):1442–1462, 2005.
- K. Draiche, A. Tounsi, and S. Mahmoud. A refined theory with stretching effect for the flexure analysis of laminated composite plates. *Geomechanics and Engineering*, 11(5):671–690, 2016.
- 380 M. D’Ottavio, L. Dozio, R. Vescovini, and O. Polit. Bending analysis of composite laminated and sandwich structures using sublaminated variable-kinematic ritz models. *Composite Structures*, 155:45–62, 2016.
- F. Ebrahimi and M. Barati. Buckling analysis of smart size-dependent higher order magneto-electro-thermo-elastic functionally graded nanosize beams. *Journal of Mechanics*, 33(1):23–33,
385 2017.
- F. Ebrahimi and N. Farazmandnia. Thermo-mechanical vibration analysis of sandwich beams with functionally graded carbon nanotube-reinforced composite face sheets based on a higher-order shear deformation beam theory. *Mechanics of Advanced Materials and Structures*, 24(10):820–829, 2017.
- 390 F. Ebrahimi and N. Shafiei. Influence of initial shear stress on the vibration behavior of single-layered graphene sheets embedded in an elastic medium based on Reddy’s higher-order shear deformation plate theory. *Mechanics of Advanced Materials and Structures*, 24(9):761–772, 2017.
- M. Filippi, A. Pagani, M. Petrolo, G. Colonna, and E. Carrera. Static and free vibration analysis
395 of laminated beams by refined theory based on Chebyshev polynomials. *Composite Structures*, 132:1248–1259, 2015.
- M. Filippi, M. Petrolo, S. Valvano, and E. Carrera. Analysis of laminated composites and sandwich structures by trigonometric, exponential and miscellaneous polynomials and a MITC9 plate element. *Composite Structures*, 150:103–114, 2016.
- 400 J. Fish. The s-version of the finite element method. *Computers & Structures*, 43(3):539–547, 1992.
- J. Fish and S. Markolefas. The s-version of the finite element method for multilayer laminates. *International Journal for Numerical Methods in Engineering*, 33(5):1081–1105, 1992.

- Q. He, H. Hu, S. Belouettar, G. Guinta, K. Yu, Y. Liu, F. Biscani, E. Carrera, and M. Potier-Ferry. Multi-scale modelling of sandwich structures using hierarchical kinematics. *Composite Structures*, 93(9):2375–2383, 2011.
- H. Hu, S. Belouettar, M. Potier-Ferry, et al. Multi-scale modelling of sandwich structures using the Arlequin method Part I: Linear modelling. *Finite Elements in Analysis and Design*, 45(1):37–51, 2008.
- 410 H. Hu, S. Belouettar, M. Potier-Ferry, A. Makradi, et al. Multi-scale nonlinear modelling of sandwich structures using the Arlequin method. *Composite Structures*, 92(2):515–522, 2010.
- S. Hühne, J. Reinoso, E. Jansen, and R. Rolfes. A two-way loose coupling procedure for investigating the buckling and damage behaviour of stiffened composite panels. *Composite Structures*, 136:513–525, 2016.
- 415 R. Jones, R. Callinan, K. Teh, and K. Brown. Analysis of multi-layer laminates using three-dimensional super-elements. *International Journal for Numerical Methods in Engineering*, 20(3):583–587, 1984.
- R. K. Kapania and S. Raciti. Recent advances in analysis of laminated beams and plates, Part I: Shear effects and buckling. *AIAA Journal*, 27(7):923–935, 1989a.
- 420 R. K. Kapania and S. Raciti. Recent advances in analysis of laminated beams and plates, Part II: Vibrations and wave propagation. *AIAA Journal*, 27(7):935–946, 1989b.
- S. Khalili, M. Shariyat, and I. Rajabi. A finite element based global–local theory for static analysis of rectangular sandwich and laminated composite plates. *Composite Structures*, 107:177–189, 2014.
- 425 M. Lezgy-Nazargah, S. Beheshti-Aval, and M. Shariyat. A refined mixed global–local finite element model for bending analysis of multi-layered rectangular composite beams with small widths. *Thin-Walled Structures*, 49(2):351–362, 2011.
- X. Li and D. Liu. A laminate theory based on global–local superposition. *International Journal for Numerical Methods in Biomedical Engineering*, 11(8):633–641, 1995.
- 430 X. Li and D. Liu. Generalized laminate theories based on double superposition hypothesis. *International Journal for Numerical Methods in Engineering*, 40(7):1197–1212, 1997.

- A. Mahi, A. Tounsi, et al. A new hyperbolic shear deformation theory for bending and free vibration analysis of isotropic, functionally graded, sandwich and laminated composite plates. *Applied Mathematical Modelling*, 39(9):2489–2508, 2015.
- 435 K. Mao and C. Sun. A refined global-local finite element analysis method. *International Journal for Numerical Methods in Engineering*, 32(1):29–43, 1991.
- H. M. Mourad, T. O. Williams, and F. L. Addessio. Finite element analysis of inelastic laminated plates using a global–local formulation with delamination. *Computer Methods in Applied Mechanics and Engineering*, 198(3):542–554, 2008.
- 440 D. Muheim Thompson and O. Hayden Griffin JR. 2-d to 3-d global/local finite element analysis of cross-ply composite laminates. *Journal of Reinforced Plastics and Composites*, 9(5):492–502, 1990.
- J. T. Oden, L. Demkowicz, W. Rachowicz, and T. Westermann. Toward a universal hp adaptive finite element strategy, Part 2. A posteriori error estimation. *Computer Methods in Applied*
445 *Mechanics and Engineering*, 77(1-2):113–180, 1989.
- A. Pagani, A. G. De Miguel, M. Petrolo, and E. Carrera. Analysis of laminated beams via Unified Formulation and Legendre polynomial expansions. *Composite Structures*, 156:78–92, 2016. 70th Anniversary of Professor J. N. Reddy.
- N. Pagano and S. Soni. Global-local laminate variational model. *International Journal of Solids*
450 *and Structures*, 19(3):207–228, 1983.
- A. Peano. Hierarchies of conforming finite elements for plane elasticity and plate bending. *Computers & Mathematics with Applications*, 2(3-4):211–224, 1976.
- W. Prager. Variational principles of linear elastostatics for discontinuous displacements, strains and stresses. *Recent Progress in Applied Mechanics. The Folkey Odquist Volume. Stockholm: Almquist and Wiksell*, pages 463–474, 1967.
- 455 J. Reddy. A simple higher-order theory for laminated composite plates. *Journal of Applied Mechanics*, 51(4):745–752, 1984a.
- J. Reddy. *An introduction to the finite element method*, volume 2. McGraw-Hill New York, 1993.
- J. Reddy and D. Robbins. Theories and computational models for composite laminates. *Applied*
460 *Mechanics Reviews*, 47(6):147–169, 1994.

- J. N. Reddy. *Energy and variational methods in applied mechanics: with an introduction to the finite element method*. Wiley New York, 1984b.
- D. Robbins and J. Reddy. Variable kinematic modelling of laminated composite plates. *International Journal for Numerical Methods in Engineering*, 39(13):2283–2317, 1996.
- 465 R. Schardt. Eine erweiterung der technischen biegetheorie zur berechnung prismatischer faltwerke. *Der Stahlbau*, 35:161–171, 1966.
- C. Sun and W. Liao. Analysis of thick section composite laminates using effective moduli. *Journal of Composite Materials*, 24(9):977–993, 1990.
- K. Surana, S. Petti, A. Ahmadi, and J. Reddy. On p-version hierarchical interpolation functions
470 for higher-order continuity finite element models. *International Journal of Computational Engineering Science*, 2(04):653–673, 2001.
- B. Szabó, A. Düster, and E. Rank. *The p-Version of the Finite Element Method*. Wiley Online Library, 2004.
- B. A. Szabó and I. Babuška. *Finite element analysis*. John Wiley & Sons, 1991.
- 475 B. A. Szabó and A. Mehta. p-convergent finite element approximations in fracture mechanics. *International Journal for Numerical Methods in Engineering*, 12(3):551–560, 1978.
- S. Timoshenko. On the transverse vibrations of bars of uniform cross-section. *The London, Edinburgh, and Dublin Philosophical Magazine and Journal of Science*, 43(253):125–131, 1922.
- S. Valvano and E. Carrera. Multilayered plate elements with node-dependent kinematics for
480 the analysis of composite and sandwich structures. *Facta Universitatis, Series: Mechanical Engineering*, 15(1):1–30, 2017.
- D. Versino, H. M. Mourad, and T. O. Williams. A global–local discontinuous galerkin shell finite element for small-deformation analysis of multi-layered composites. *Computer Methods in Applied Mechanics and Engineering*, 271:269–295, 2014.
- 485 D. Versino, H. M. Mourad, T. O. Williams, and F. L. Addessio. A global–local discontinuous galerkin finite element for finite-deformation analysis of multilayered shells. *Computer Methods in Applied Mechanics and Engineering*, 283:1401–1424, 2015.
- V. Z. Vlasov. *Thin-walled elastic beams*. National Technical Information Service, 1984.

- C. Wenzel, P. Vidal, M. D'Ottavio, and O. Polit. Coupling of heterogeneous kinematics and
490 finite element approximations applied to composite beam structures. *Composite Structures*,
116:177–192, 2014.
- J. D. Whitcomb and K. Woo. Application of iterative global/local finite-element analysis. Part
1: Linear analysis. *International Journal for Numerical Methods in Biomedical Engineering*,
9(9):745–756, 1993a.
- 495 J. D. Whitcomb and K. Woo. Application of iterative global/local finite-element analysis. Part 2:
Geometrically non-linear analysis. *International Journal for Numerical Methods in Biomedical
Engineering*, 9(9):757–766, 1993b.
- T. O. Williams. A generalized multilength scale nonlinear composite plate theory with delami-
nation. *International Journal of Solids and Structures*, 36(20):3015–3050, 1999.
- 500 E. Zappino, G. Li, A. Pagani, and E. Carrera. Global-local analysis of laminated plates by node-
dependent kinematic finite elements with variable ESL/LW capabilities. *Composite Structures*,
172:1–14, 2017.
- E. Zappino, G. Li, and E. Carrera. Node-dependent kinematic elements for the dynamic analysis
of beams with piezo-patches. *Journal of Intelligent Material Systems and Structures*, 29(16):
505 3333–3345, 2018.
- J. Zhu and O. Zienkiewicz. Adaptive techniques in the finite element method. *International
Journal for Numerical Methods in Biomedical Engineering*, 4(2):197–204, 1988.
- O. Zienkiewicz and J. Z. Zhu. A simple error estimator and adaptive procedure for practical
engineering analysis. *International Journal for Numerical Methods in Engineering*, 24(2):337–
510 357, 1987.
- O. Zienkiewicz, J. D. S. Gago, and D. W. Kelly. The hierarchical concept in finite element
analysis. *Computers & Structures*, 16(1):53–65, 1983.
- O. Zienkiewicz, J. Zhu, and N. Gong. Effective and practical h–p-version adaptive analysis
procedures for the finite element method. *International Journal for Numerical Methods in
515 Engineering*, 28(4):879–891, 1989.